

# Identification of Inhibitors of Cholesterol Transport Proteins Through the Synthesis of a Diverse, Sterol-Inspired Compound Collection

**Whitmarsh-Everiss, Thomas; Olsen, Asger Hegelund; Laraia, Luca**

*Published in:*
Angewandte Chemie International Edition

*Link to article, DOI:*
10.1002/anie.202111639

*Publication date:*
2021

*Document Version*
Peer reviewed version

A Journal of the Gesellschaft Deutscher Chemiker

Angewandte International Edition GDCh Chemie

www.angewandte.org

## Accepted Article

**Title:** Identification of inhibitors of cholesterol transport proteins through the synthesis of a diverse, sterol-inspired compound collection

**Authors:** Luca Laraia, Thomas Whitmarsh-Everiss, and Asger Hegelund Olsen



**To be cited as:** *Angew. Chem. Int. Ed.* 10.1002/anie.202111639

**Link to VoR:** https://doi.org/10.1002/anie.202111639

WILEY-VCH

10.1002/anie.202111639

WILEY-VCH

RESEARCH ARTICLE

# Identification of inhibitors of cholesterol transport proteins through the synthesis of a diverse, sterol-inspired compound collection

Thomas Whitmarsh-Everiss, Asger Hegelund Olsen, and Luca Laraia*[a]

[a] T. Whitmarsh-Everiss, A. H. Olsen, L. Laraia
Department of Chemistry
Technical University of Denmark
Kemitorvet 207, 2800 Kongens Lyngby, Denmark
E-mail: luclar@kemi.dtu.dk

Supporting information for this article is given via a link at the end of the document.

**Abstract:** Cholesterol transport proteins regulate a vast array of cellular processes including lipid metabolism, vesicular and non-vesicular trafficking, organelle contact sites, and autophagy. Despite their undoubted importance, the identification of selective modulators of this class of proteins has been challenging due to the structural similarities in the cholesterol-binding site. Herein we report a general strategy for the identification of selective inhibitors of cholesterol transport proteins *via* the synthesis of a diverse sterol-inspired compound collection. Fusion of a primary sterol fragment to an array of secondary privileged scaffolds led to the identification of potent and selective inhibitors of the cholesterol transport protein Aster-C, which displayed a surprising preference for the unnatural sterol AB-ring stereochemistry, and new inhibitors of Aster-A. We propose that this strategy can, and should be applied to any therapeutically relevant sterol-binding protein

## Introduction

Cholesterol transport proteins (CTPs) play important roles in vesicular and non-vesicular cholesterol trafficking, reflected by differences in both their subcellular localisation and sterol binding capabilities.[1] Major known classes of CTPs include the oxysterol-binding protein (OSBP)-related proteins (ORPs), the steroidogenic acute regulatory protein (StAR)-related lipid transfer (START)-related domain (STARD) proteins, the Aster proteins, and the Niemann-Pick type C proteins.[1] In addition to their roles in cholesterol transport, CTPs have been demonstrated to regulate organelle contact sites, cellular metabolism, degradative pathways such as autophagy, and viral entry.[2–7] CTPs have thus been implicated and proposed as targets for the treatment of neurodegenerative disorders, viral infections, as well as numerous types of cancer. Despite the clear biological importance of these CTPs, very few selective inhibitors of these proteins are known, in part due to the inherent difficulties of targeting their structurally related cholesterol binding domains. Therefore, the identification of selective inhibitors of CTPs would enable the further study and therapeutic targeting of sterol-mediated processes. The identification of novel bioactive small molecules has in recent years seen a trend towards the use of natural product (NP)-like collections of high predicted biological diversity.[8] As such, a number of techniques to afford NP-like and diverse compound collections have been described including diversity-oriented synthesis (DOS)[9,10], biology-oriented synthesis (BIOS)[11], complexity-to-diversity (CtD)[12], function-oriented synthesis[13], and fragment-based designs[14] in addition to the pseudo-natural product approach[15,16]. Inspired by these techniques, we hypothesised that a focussed compound collection enriched in selective hits against different CTPs could be synthesised by the fusion of a privileged sterol-like scaffold to a diverse array of heterocyclic fragments commonly encountered in a range of NPs. Herein, we report the design and synthesis of a sterol-inspired compound collection composed of diverse sterol AB ring-heterocyclic fusions. Using the Aster family of proteins, we demonstrate the suitability of our sterol-inspired library as a source of lead compounds against CTPs. Using differential scanning fluorimetry (DSF), fluorescence polarisation (FP) and cholesterol transport assays, we identify a series of pyrazole-sterol fusions that selectively inhibit Aster-C in addition to two new Aster-A inhibitor chemotypes.

## Results and Discussion

The design of a sterol-inspired compound collection began with the selection of an appropriate primary scaffold that would be representative of the sterol AB-ring system. This was predicted to function as a “bait” to engage sterol-binding proteins. One key requirement of this scaffold was that it had to allow the fusion of heterocyclic secondary scaffolds, which should confer selectivity between structurally related targets, and should ideally be accessible in a limited number of synthetic steps. We identified the saturated *trans*-fused hydroxy-decalin system as a suitable primary scaffold, owing to its previous use in a proteomic based mapping of cholesterol-interacting proteins[17] in addition to its occurrence in a range of sterols (Figure 1). This would then be coupled to secondary scaffolds predominantly, but not exclusively, found in natural products. Ultimately, we decided upon the *trans*-fused decalone **1** (Scheme 1) to serve as the core building block for library synthesis. Exploiting the inherent reactivity of its C9 ketone, we anticipated that a diverse range of heterocycle-fused compounds could be synthesised – either directly from decalone **1** or from readily accessible intermediates. We also established additional guidelines to guide our synthesis efforts. For each scaffold series, we set out to synthesise at least three analogues featuring different substitution patterns of both electron donating and electron withdrawing groups, intending to obtain preliminary structure-activity relationships (SAR) of putative hits arising from biological testing. Secondly, we chose to synthesise the

10.1002/anie.202111639
WILEY-VCH

RESEARCH ARTICLE

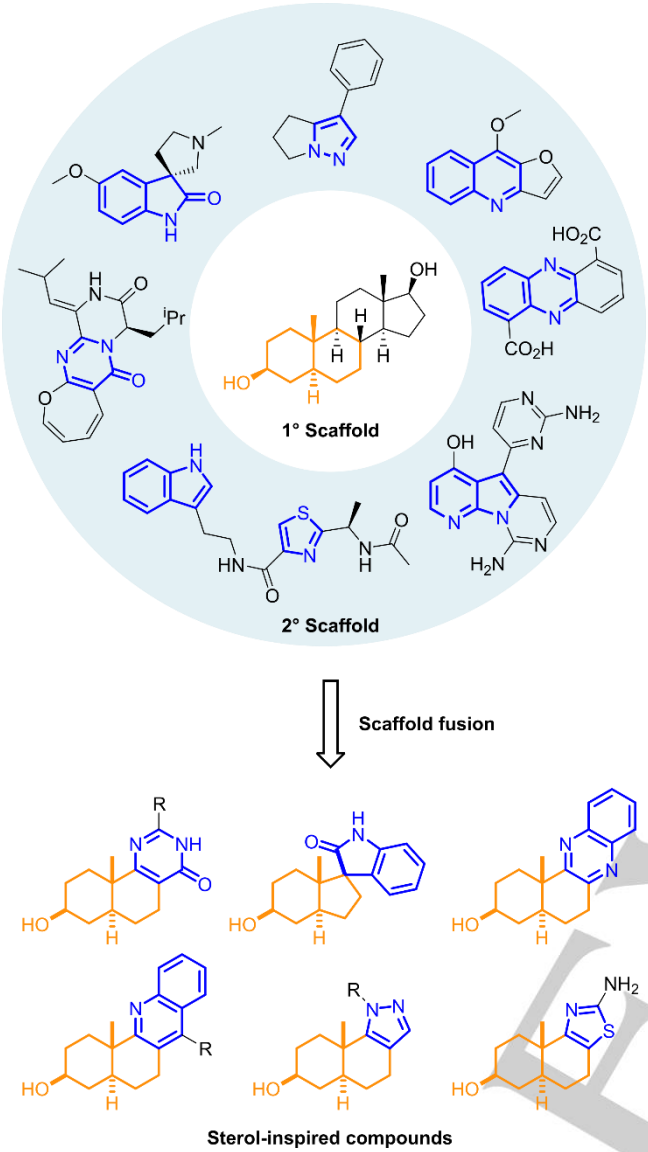


**Figure 1.** Design of sterol-inspired compounds. Fusion of a primary sterol-derived scaffold comprising the AB ring system (orange) with secondary heterocyclic scaffolds encountered in a diverse range of natural products (blue) affords a sterol-inspired compound collection

compound collection in a racemic manner, thereby effectively doubling the size of our screening collection and including both the naturally occurring and opposite enantiomers of the core sterol primary scaffold.

Synthesis began with the construction of trans-fused decalone **1**. This was synthesised in six steps from commercial starting materials *via* the known Wieland-Miescher ketone (WMK), affording decalone **1** in an overall yield of 37% (Supplementary scheme S1). To further the scaffold diversity of our sterol-inspired collection, a series of intermediate compounds were synthesised that allowed access to further heterocycle fusions, namely α-bromoketone **2**, hydroxymethylenes **3** and **4**, and β-ketoester **5** (Supplementary scheme S2). A number of heterocyclic analogues were accessed directly from ketone 1 in one step (Scheme 1a). Quinoline fused analogues **6a** – **6i** were synthesised by a Friedländer synthesis via condensation with the in situ generated 2-aminobenzaldehyde and subsequent base-promoted cyclisation.

In an analogous manner, ketone **1** was reacted with a series of 2-aminobenzo or 2-aminoacetophenones under acidic conditions, affording a complementary series of quinoline analogues **7a** – **7h** featuring alkyl and aryl substituents at the C14 position. Indole fused analogues **8a** – **8g** and 7-azaindole fused analogues **9a** – **9c** were obtained via the Fischer-indole synthesis from the corresponding arylphenylhydrazines and 2-hydrazinopyridines respectively. The ring-expanded lactam **10** was synthesised via a Beckmann rearrangement with hydroxylamine-O-sulfonic acid in glacial acetic acid, proceeding with acetylation of the C3 hydroxyl group. Additionally, spirocyclic dihydroquinazolinones **11a** – **11b** were synthesised by reaction with 2-aminobenzamides, yielding the products as inseparable mixtures of diastereoisomers. From α-bromoketone **2** (Scheme 1b), imidazothiadiazole analogues **12a** – **12b** were synthesised by the microwave-assisted reaction with 2-aminothiadiazoles in ethanol. Under similar conditions, thiazole fused analogues **13a** – **13d** were afforded by reaction of either substituted thioamides or with thiourea. Lastly, quinoxaline fused analogue **14** was accessed by reaction with o-phenylenediamine.

The methoxyethoxymethyl (MEM) ether-protected hydroxymethylene **3** was reacted with a series of substituted phenylhydrazines to yield mixtures of regioisomeric pyrazole-fused analogues (Scheme 1c). Acid-mediated deprotection of the MEM group allowed for separation of these regioisomeric mixtures by preparative HPLC, affording the angular pyrazoles **15a** – **15e** as major products and the linear pyrazoles **16a** – **16c** as the minor products. Interestingly, the 2-fluorophenyl substituted pyrazole **15d** was found to exist as a mixture of conformational isomers due to restricted rotation around the pyrazole-phenyl group N-C bond (Supplementary figure S3). Similarly, pairs of regioisomeric pyrazolopyrimidine fused analogues were synthesised through reaction of unprotected hydroxymethylene **4** and 2-aminopyrazoles affording angular analogues **17a** – **17e** and linear fused analogues **18a** – **18e** as the major and minor products respectively. Reaction of hydroxymethylenes **3** and **4** with the dinucleophilic hydrazine hydrate and hydroxylamine hydrochloride respectively, yielded the unsubstituted pyrazole and isoxazole analogues **19** and **20**. Condensation and cyclisation of various substituted amidines with β-ketoester **5** and subsequent MEM-deprotection successfully afforded pyrimidone fused analogues **21a** – **21e** in good yields over two steps (Scheme 1d). Finally, spirocyclic ring-contracted oxindoles **22a** – **22c** were accessed with complete diastereoselectivity via a one-pot bromination and acid promoted semi-pinacol rearrangement of indole fused analogues **8a** – **8c** (Scheme 1e).

In total, 65 sterol-inspired compounds (Supplementary figure S4) were synthesised for use in biological screening, featuring 14 distinct secondary heterocyclic scaffolds of which 11 can be classed as pseudo-natural products. Cheminformatics analysis revealed that the compound collection displayed a similar NP-likeness and shape diversity profile to previously reported pseudo-NP collections (see Supplementary Figure S5 and accompanying discussion). Furthermore, a novelty analysis confirmed that none of the scaffold combinations are known in the academic literature, while only distantly related scaffolds are found in the patent literature.

In order to evaluate the suitability of our sterol-inspired library as a source of leads against sterol-transfer proteins, we chose to target the Aster family of CTPs. The Asters (Asters-A, B,

10.1002/anie.202111639





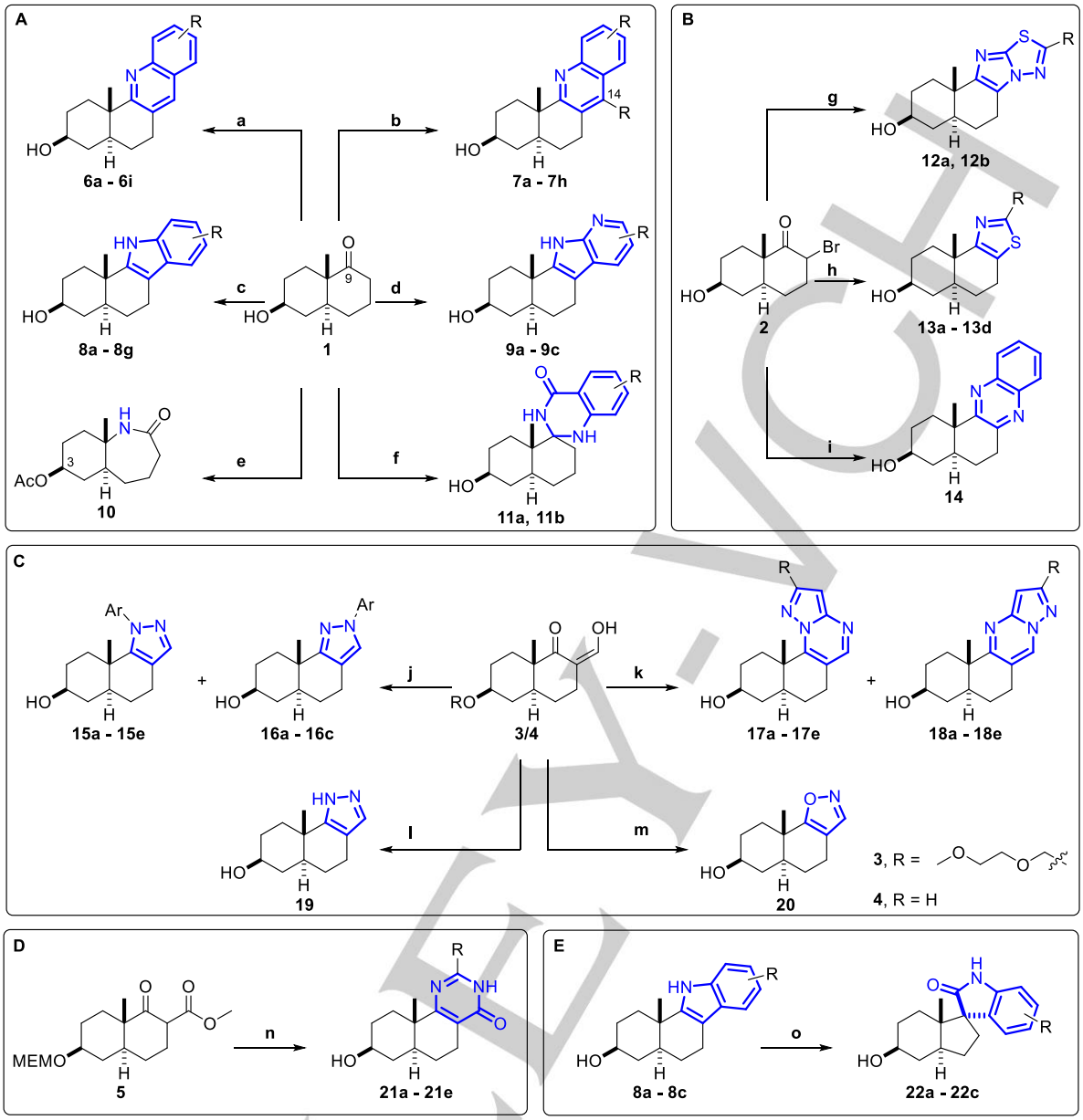


**Scheme 1. Synthesis of the sterol-inspired compound library. A)** Analogue synthesis from ketone **1**. a) 2-nitrobenzaldehyde, Fe/HCl (0.1M aq.), EtOH 78 °C then ketone, KOH, 70 °C, 24 – 56%; b) 2-aminoacetophenone/benzophenone, *p*-TsOH.$H_2O$, 110 °C (μwave), 2 h, 44 – 79%; c) hydrazinopyridine HCl, diethylene glycol, 250 °C (μwave), 3 h, 10 – 39%; d) phenylhydrazine HCl, *p*-TsOH.$H_2O$, 78 °C, 35 – 72%; e) hydroxylamine-*O*-sulfonic acid, AcOH, 120 °C (μwave), 1 h, 34%; f) 2-aminobenzamide, $NH_4Cl$, EtOH, 78 °C, 32 h, 18 – 80%. **B)** Analogue synthesis from bromoketone **30**. g) aminothiadiazole, EtOH, 150 °C (μwave), 2 h, 36 – 39%; h) thiourea, EtOH, 78 °C, 26 – 61%; i) o-phenylenediamine, EtOH, 78 °C, 3 d, 3%. **C)** Analogue synthesis from hydroxymethylenes **38**/**39**. j) phenylhydrazine HCl, MeOH:AcOH (4:1), r.t., then HCl (6M aq.), THF, r.t., 18 h, 5 – 47% (2 steps); k) aminopyrazole, *p*-TsOH.$H_2O$, toluene, 116 °C, 2 h, 21 – 26%; l) hydrazine hydrate, AcOH, reflux, 3 h, 27%; m) $NH_2OH.HCl$, EtOH, 78 °C, 2 h, 60%. **D)** Analogue synthesis from β-ketoester **60**. n) amidine, $K_2CO_3$, MeOH, 66 °C, 24 h, 74 – 90% then HCl (6M aq.), THF, r.t., 24 h, 48 – 90%. **E)** Analogue synthesis from indoles **20 – 22**. o) NBS, AcOH:THF:$H_2O$ (1:1:1), r.t., 30 min, 45 – 88%

and C, also known as GRAMD1A, B, and C respectively) are a family of sterol transfer proteins responsible for the transport of cholesterol between plasma membranes (PM) and the endoplasmic reticulum (ER).[18] The roles of the Aster proteins in autophagosome biogenesis[19], lysosomal trafficking and mTORC1 signalling[20], as well as mitochondrial cholesterol transport[21] have recently been elucidated, however their functional redundancy and relevance as drug targets still remains to be determined. Whilst highly selective inhibitors of Aster-A are known[19], inhibitors of Aster-B and Aster-C have also been identified but suffer from poor selectivity.[22] Identification of compounds that both selectively and potently inhibit Aster-B and Aster-C would allow one to individually probe the Aster proteins, facilitating the study of their specific roles without incurring into functional redundancy, which has previously been observed when using genetic methods to perturb the Aster proteins. With this in mind, an ideal lead compound should be at least 10-fold selective within the Aster family and display potential for further improvement. This would ultimately enable us to exploit such a compound for therapeutic purposes. We commenced our screening efforts with a DSF assay[19], investigating whether the sterol-inspired compounds were able to

10.1002/anie.202111639




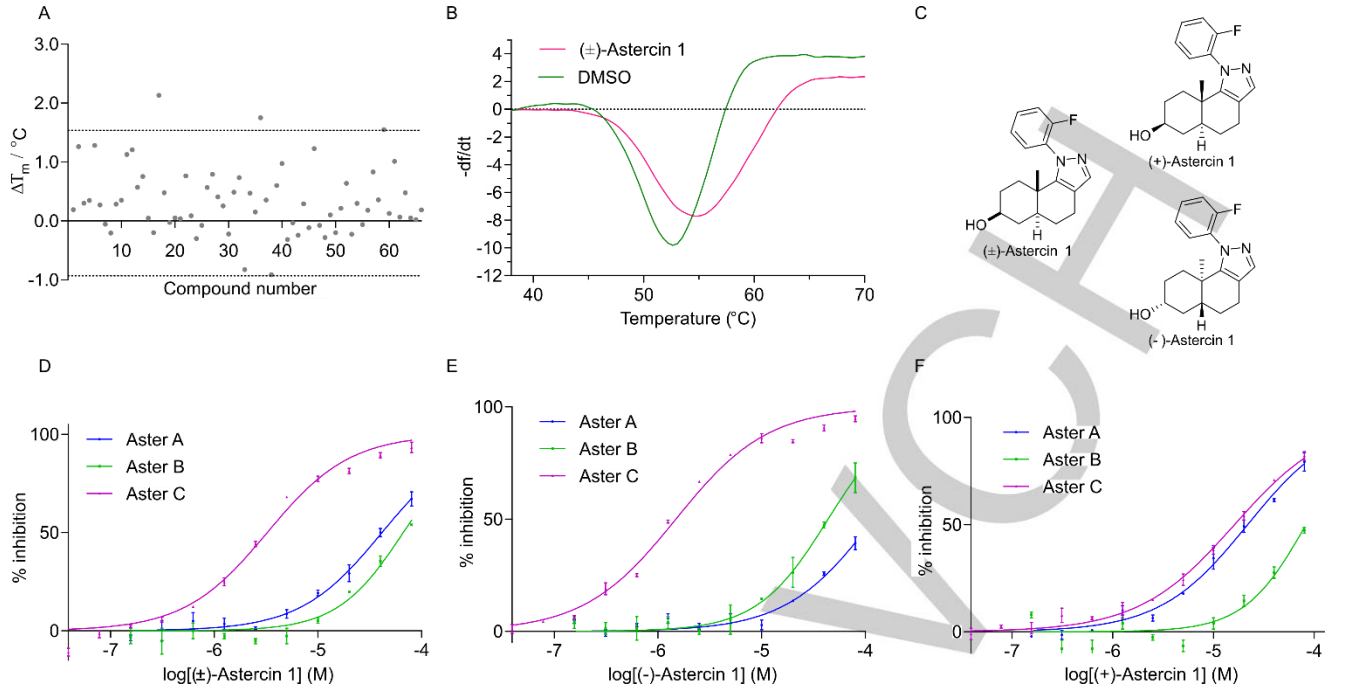


**Figure 2.** DSF and FP screening data of the sterol-inspired compound collection. **A** DSF screening plot of the sterol-inspired collection against Aster-C ASTER domain. Data shown are averages of two replicates. Hit cut-off set as ± two s.d. from the mean $T_m$ of the library. **B** Protein melting curves for the thermal-stabilisation of Aster C ASTER domain induced by Astercin 1. **C** Structures of (±), (+), and (-)-Astercin 1. **D** Fluorescence polarisation assay selectivity of (±)-Astercin 1 against ASTER domains of Asters A, B, and C. **E** Fluorescence polarisation assay selectivity of (-)-Astercin 1 against ASTER domains of Asters A, B, and C. **F** Fluorescence polarisation assay selectivity of (+)-Astercin 1 against Aster domains of Asters A, B, and C. Fluorescence polarisation data shown are reported as the mean ± SEM of an individual experiment run in either duplicate or triplicate.

stabilise the purified ASTER domains of Asters-A, B, and C towards thermal denaturation. The library was tested at a single concentration of 50 µM and hits selected using upper and lower cut-offs of ± 2 standard deviations from the mean melting temperature ($T_m$) of the whole library. With these cut-offs, eight compounds were identified that significantly stabilised the ASTER domains towards heating compared to the negative control; representing an overall hit rate of 9% for the compound library (Figures 2a,b, Table 1, and supplementary figures S6, S7). Only two compounds were found to target more than one Aster protein, providing initial evidence that selectivity between structurally similar proteins can be achieved with our approach. To further investigate the activity of our initial hit compounds and to validate their binding to the ASTER domain, all hits were screened in an FP assay. The FP assay was performed in a competitive inhibition mode against 22-NBD-cholesterol, a fluorescent cholesterol derivative previously reported to bind the Aster proteins with high affinity[19]. Inhibition against their primary target was observed for five of the six hits selected from the DSF screen. Subsequently, validated hits were screened against the other Aster proteins to determine their selectivity. Initially, angular pyrazoles **15c** and **15d**, hits against Aster-C (Table 1, $IC_{50}$ = 3.89 ± 0.32 µM and 2.29 ± 1.10 µM respectively), were identified as having promising selectivity profiles, with **15d** (which we have named (±)-Astercin 1) showing over 15-fold selectivity for Aster-C over Aster-A and 30-fold selectivity over Aster-B (Figure 2d).

The remaining members of the angular pyrazole series that were not previously identified as hits in the DSF assay were rescreened in the FP assay. Analogues **15a** and **15b** were identified as hits with moderate potency ($IC_{50}$ = 7.42 ± 3.04 µM and 6.44 ± 1.86 µM, respectively) against Aster-C (Table 1). This finding suggests that for smaller focussed collections, such as the sterol-inspired collection, the threshold for hit selection could be lowered in order to include true-positives in subsequent assays. Despite this, we were still able to observe a positive correlation between observed $\Delta T_m$ in the DSF assay and $IC_{50}$ values determined by FP. In addition to the Aster-C inhibitors, two linear pyrazolopyrimidine analogues **18a** and **18b**, which were identified as hits against Aster-A alongside the imidazothiadiazole analogue **12a**, showed moderate selectivity over Aster-C and complete selectivity over Aster-B (Table 1), thus representing promising new classes of Aster-A inhibitors. Unfortunately, we were unable to validate angular pyrazolopyrimidine **17c** as a hit against Aster-B, suggesting the importance of hydroxyl substitution to achieve high potency against Aster-B as per the known non-selective cholesterol transport inhibitor U18666A (Supplementary figure S7).[22] In line with our aim of synthesising our compound library to generate preliminary SAR information for hit compounds, we could observe a clear trend in the potency of the pyrazole fused Aster-C inhibitors. (Table 1). The unsubstituted pyrazole **19** and isomeric linear pyrazoles **16a** – **16c** were found to be inactive in both the DSF and FP assays (data not shown), highlighting the importance of both phenyl substitution of the pyrazole and its relative positioning in the ASTER domain binding site. Inactivity from 3,5-disubstituted **15e** (entry 8) suggests the binding site of Aster-C is incompatible with this substitution pattern, whereas substitution at both the 2- and 4- positions is well tolerated (entries 2 – 5). This early SAR provides invaluable information to guide future optimisation efforts of the pyrazole fused analogues as Aster-C inhibitors.

With this SAR data in hand, we sought to identify the active enantiomer of (±)-Astercin 1, and additionally gain insight into the stereochemical preference of the ASTER domain

**Table 1.** Change in melting temperature ($\Delta T_m$) from DSF assays and $IC_{50}$ values determined from FP experiments of sterol-inspired compounds against purified ASTER domains of Asters-A, B, and C.

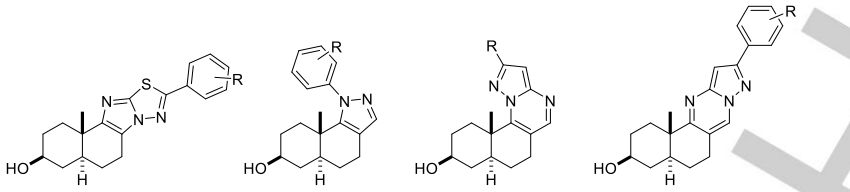

12 15 17 18

| Entry | Compound | R | Aster-A | | Aster-B | | Aster-C | |
|---|---|---|---|---|---|---|---|---|
| | | | $\Delta T_m$ (°C)[a] | $IC_{50}$ (μM)[b] | $\Delta T_m$ (°C)[a] | $IC_{50}$ (μM)[b] | $\Delta T_m$ (°C)[a] | $IC_{50}$ (μM)[b] |
| 1 | 12a | 4-OMe | 5.10 | 1.62 ± 0.25 | 0.96 | nd | 0.79 | 3.69 ± 0.91 |
| 2 | 15a | H | 0.46 | nd | 0.74 | nd | 1.13 | 7.42 ± 3.04 |
| 3 | 15b | 4-OMe | 1.23 | nd | 0.96 | nd | 1.28 | 6.44 ± 1.86 |
| 4 | 15c | 4-Cl | 0.92 | > 20 | 0.87 | > 20 | 1.75 | 3.89 ± 0.32 |
| 5 | 15d ((±)-Astercin 1) | 2-F | 0.97 | 42.3 ± 1.14 | 0.95 | 68.0 ± 4.31 | 2.13 | 2.29 ± 1.10 |
| 6 | (-)-Astercin 1 | 2-F | nd | > 80 | nd | 46.8 ± 5.78 | nd | 1.51 ± 0.56 |
| 7 | (+)-Astercin 1 | 2-F | nd | 23.0 ± 1.16 | nd | 78.0 ± 4.26 | nd | 16.9 ± 5.41 |
| 8 | 15e | 3,5-Me | 0.41 | nd | 0.53 | nd | 0.05 | nd |
| 9 | 17c | *i*-Pr | 1.02 | nd | 1.50 | > 20[c] | 1.50 | nd |
| 10 | 18a | H | 3.30 | 6.59 ± 0.35 | 1.80 | > 20 | 1.26 | > 20 |
| 11 | 18b | 4-OMe | 5.50 | 1.23 ± 0.23 | 0.97 | > 20[c] | 1.21 | ~15[d] |
| 12 | Autogramin-2 | N/A | nd | 1.93 ± 1.06 | nd | > 20[c] | nd | > 20 |
| 13 | AI-1l | N/A | nd | > 20 | nd | > 20 | nd | 4.81 ± 1.49[e] |
| 14 | U18666A | N/A | nd | nd | nd | 1.05 ± 0.45 | nd | nd |

[a] $\Delta T_m$ values are reported as the mean of two replicates. [b] $IC_{50}$ values reported as mean ± s.d. of three individual experiments run in triplicate. [c] No inhibition observed. [d] Value is approximate owing to solubility problems at concentrations > 10 μM [e] Data were seen to plateau at ~60 % inhibition, see supporting information for FP curves

binding sites. Utilising reported organocatalytic procedures[23,24] to access enantioenriched (*S*) and (*R*)-WMK, decalones (-)-**1** and (+)-**1** were synthesised in an identical manner to (±)-**1**. In an optimised procedure, both (+)-Astercin 1 and (-)-Astercin 1 were successively synthesised from decalones (-)-**1** and (+)-**1** (Supplementary scheme S3). In synthesising (+) and (-)-Astercin 1, we chose to protect the secondary hydroxyl group as a TBS ether due to its comparative ease of removal compared to MEM ethers. Using modified conditions[25] to synthesise the sterol-pyrazole fusion, we were able to efficiently access (+) and (-)-Astercin 1 in a one-pot sequence from the corresponding (+) and (-)-TBS hydroxymethylenes.

Subsequently, (±), (+), and (-)-Astercin 1 were screened in the FP assay against Aster-C with (-)-Astercin 1, the enantiomer featuring "unnatural" AB-ring stereochemistry identified as the active enantiomer over (+)-Astercin 1 (Table 1, figure 2e,f, $IC_{50}$ = 1.51 ± 0.56 μM and $IC_{50}$ = 16.9 μM respectively). Further profiling against Asters-A and B showed that (-)-Astercin 1 was 30-fold selective for Aster-C over Aster-B and >50-fold selective for Aster-C over Aster-A (Table 1, $IC_{50}$ = 46.8 μM ± 5.78 μM and $IC_{50}$ > 80 μM). Interestingly, (+)-Astercin 1 was found to have higher potency against Aster-A (Table 1, $IC_{50}$ = 23.0 ± 1.16 μM) than (-)-Astercin 1, suggesting a reversal in the stereochemical preference of Aster-A to bind the "natural" sterol AB-ring stereochemistry over Aster-B or Aster-C. This preference could provide a plausible way to exploit the AB-ring stereochemistry to engineer family selectivity within one class of Aster inhibitors.

Following the recent discovery of a 20α-hydroxycholesterol derived Aster-C modulator[22] AI-1l, we sought to benchmark (-)-Astercin 1 against it. (-)-Astercin 1 was over 3-fold more potent than AI-1l ($IC_{50}$ = 4.81 ± 1.49 μM, though FP data did not plateau at 100% inhibition in our assay using human ASTER domains) towards Aster-C, with AI-1l displaying a moderate selectivity-profile against Aster-A and -B (Supplementary figure S7). Notably, AI-1l has also been reported to modulate hedgehog signalling[26] in addition to inhibiting sterol regulatory element binding protein 2 (SREBP2) processing[22], suggesting that its selectively profile will need to be evaluated further.

To further validate the ability of Astercin 1 to inhibit Aster-mediated sterol transfer, we adapted a FRET-based liposomal cholesterol transfer assay[19] to a microplate format[27] (Figure 3a – d). This assay monitors the disruption of the 23-BODIPY-cholesterol (BODIPY-Chol) and rhodamine 1,2-dihexadecanoyl-sn-glycero-3-phosphoethanolamine (Rh-DHPE) FRET pair caused by Aster-mediated transport of BODIPY-chol into acceptor liposomes prepared without any fluorescently labelled lipids. For both Aster-A and Aster-B, no significant inhibition of cholesterol transfer was observed relative to the DMSO control upon treatment with (±)-Astercin 1, in contrast to control inhibitors autogramin-2 and U18666A (Figures 3b,c). Pleasingly, the Astercin 1 selectivity profile determined via the FP assay was comparable to the compounds ability to inhibit Aster-C mediated cholesterol transfer, with (-)-Astercin 1 inhibiting transport, while (+)-Astercin 1 did not (Figure 3d).

## Conclusion

In summary, we have designed a collection of 65 sterol-inspired compounds enriched in activity against CTPs through the fusion of a steroidal primary scaffold to a diverse set of heterocyclic secondary scaffolds. Screening of the library against the Aster proteins in DSF, FP, and FRET-based assays resulted in the identification of a pyrazole fused class of selective Aster-C inhibitors, including (-)-Astercin 1, the most potent and selective Aster-C inhibitor to date. Through the synthesis of both (+) and

10.1002/anie.202111639




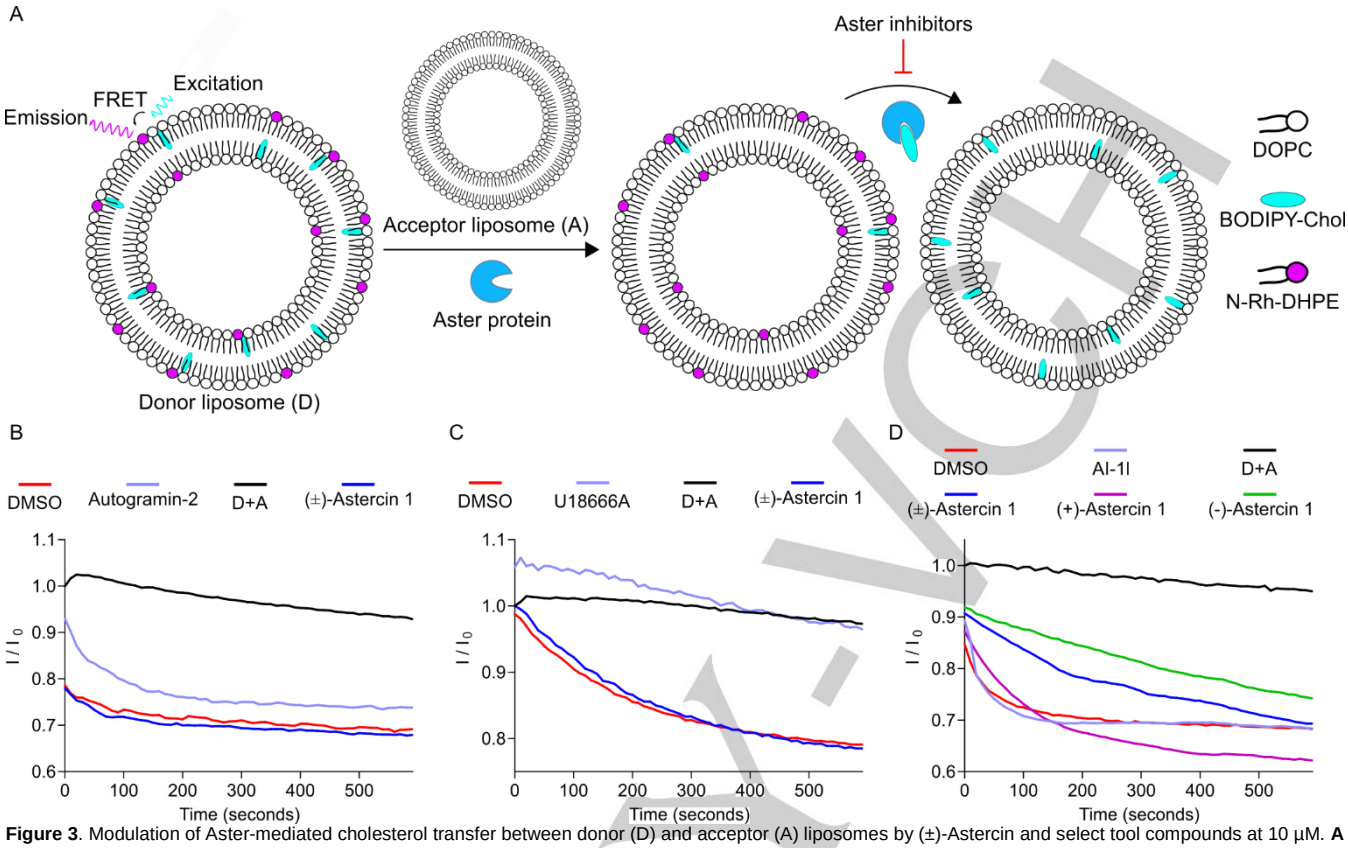


**Figure 3**. Modulation of Aster-mediated cholesterol transfer between donor (D) and acceptor (A) liposomes by (±)-Astercin and select tool compounds at 10 µM. **A** Donor liposomes containing the fluorescent lipids N-Rh-DHPE and BODIPY-Chol exhibit a strong FRET signal upon irradiation at 488 nm. Upon mixing with acceptor liposomes and Aster protein ASTER domains, BODIPY-Chol is transported to acceptor liposomes resulting in a decrease in FRET signal over time. Inhibition of the ASTER domains by small molecules slows the decrease in FRET signal. **B** Modulation of Aster-A mediated cholesterol transfer by (±)-Astercin 1 and Autogramin-2. **C** Modulation of Aster-B mediated cholesterol transfer by (±)-Astercin 1 and U18666A. **D** Modulation of Aster-C mediated cholesterol transfer by (±)-Astercin 1, (+)-Astercin 1, (-)-Astercin 1, and AI-1I. Representative data from one experiment carried out in duplicate shown (overall n=3, *N* = 2). Data was normalised to the initial fluorescence signal of the liposome donor+acceptor control. DOPC = 1,2-dioleoyl-sn-glycero-3-phosphocholine

(-)-Astercin 1, we also identified a clear stereochemical preference for the sterol AB-ring within the Aster protein family. Additionally, two new classes of Aster-A inhibitors with moderate selectivity over Aster-C were identified, giving an overall hit rate of 9% for our focussed library. (-)-Astercin 1 and its derivatives could prove to become important tool compounds for use in the study of Aster-C mediated cholesterol transport, and our newly developed strategy may be expanded to other CTPs and sterol binding proteins in the future.

## Acknowledgements

We gratefully acknowledge the Novo Nordisk Foundation (NNF17OC0028366 and NNF19OC0055818), Independent Research Fund Denmark (9041-00241B and 9041-00248B), the Carlsberg Foundation (CF19-0072), and DTU for financial support to LL. TWE acknowledges DTU for a PhD fellowship. We also thank Dr. Kasper Enemark-Rasmussen and Charlie Johansen for assistance with NMR experiments and HRMS-acquisition, respectively. Christoffer Wrist-Jensen, Magnus Bonnevie, Razan Mearraoui, and Anna Bønke are thanked for the synthesis of several sterol-fused analogues. We thank David Frej Nielsen for support with protein expression and purification.

**Keywords:** Cholesterol transport proteins • Inhibitors • Natural products • Library synthesis

[1] J. Luo, L.-Y. Jiang, H. Yang, B.-L. Song, *Trends Biochem. Sci.* **2019**, *44*, 273–292.
[2] S. Raychaudhuri, W. A. Prinz, *Annu. Rev. Cell Dev. Biol.* **2010**, *26*, 157–177.
[3] J. Wollam, A. Antebi, *Annu. Rev. Biochem.* **2011**, *80*, 885–916.
[4] R. H. Wijdeven, H. Janssen, L. Nahidiazar, L. Janssen, K. Jalink, I. Berlin, J. Neefjes, *Nat. Commun.* **2016**, *7*, 11808.
[5] M. Côté, J. Misasi, T. Ren, A. Bruchez, K. Lee, C. M. Filone, L. Hensley, Q. Li, D. Ory, K. Chandran, J. Cunningham, *Nature* **2011**, *477*, 344–348.
[6] L. Albulescu, J. Bigay, B. Biswas, M. Weber-Boyvat, C. M. Dorobantu, L. Delang, H. M. van der Schaar, Y.-S. Jung, J. Neyts, V. M. Olkkonen, F. J. M. van Kuppeveld, J. R. P. M. Strating, *Antiviral Res.* **2017**, *140*, 37–44.
[7] T. Whitmarsh-Everiss, L. Laraia, *Nat. Chem. Biol.* **2021**, *17*, 653–664.
[8] I. Pavlinov, E. M. Gerlach, L. N. Aldrich, *Org. Biomol. Chem.* **2019**, *17*, 1608–1623.
[9] S. Oh, S. B. Park, *Chem. Commun.* **2011**, *47*, 12754–12761.
[10] W. R. J. D. Galloway, A. Isidro-Llobet, D. R. Spring, *Nat. Commun.* **2010**, *1*, 80.
[11] S. Wetzel, R. S. Bon, K. Kumar, H. Waldmann, *Angew. Chemie Int. Ed.* **2011**, *50*, 10800–10826.
[12] R. W. Huigens III, K. C. Morrison, R. W. Hicklin, T. A. Flood Jr, M. F. Richter, P. J. Hergenrother, *Nat. Chem.* **2013**, *5*, 195–202.
[13] P. A. Wender, V. A. Verma, T. J. Paxton, T. H. Pillow, *Acc. Chem. Res.* **2008**, *41*, 40–49.
[14] R. A. Lowe, D. Taylor, K. Chibale, A. Nelson, S. P. Marsden, *Bioorg. Med. Chem.* **2020**, *28*, 115442.
[15] G. Karageorgis, D. J. Foley, L. Laraia, H. Waldmann, *Nat. Chem.* **2020**, *12*, 227–235.

10.1002/anie.202111639





[16] G. Karageorgis, D. J. Foley, L. Laraia, S. Brakmann, H. Waldmann, *Angew. Chemie - Int. Ed.* **2021**, *60*, 15705–15723.

[17] J. J. Hulce, A. B. Cognetta, M. J. Niphakis, S. E. Tully, B. F. Cravatt, *Nat. Methods* **2013**, *10*, 259–264.

[18] J. Sandhu, S. Li, L. Fairall, S. G. Pfisterer, J. E. Gurnett, X. Xiao, T. A. Weston, D. Vashi, A. Ferrari, J. L. Orozco, C. L. Hartman, D. Strugatsky, S. D. Lee, C. He, C. Hong, H. Jiang, L. A. Bentolila, A. T. Gatta, T. P. Levine, A. Ferng, R. Lee, D. A. Ford, S. G. Young, E. Ikonen, J. W. R. Schwabe, P. Tontonoz, *Cell* **2018**, *175*, 514-529.e20.

[19] L. Laraia, A. Friese, D. P. Corkery, G. Konstantinidis, N. Erwin, W. Hofer, H. Karatas, L. Klewer, A. Brockmeyer, M. Metz, B. Schölermann, M. Dwivedi, L. Li, P. Rios-Munoz, M. Köhn, R. Winter, I. R. Vetter, S. Ziegler, P. Janning, Y.-W. Wu, H. Waldmann, *Nat. Chem. Biol.* **2019**, *15*, 710–720.

[20] J. Zhang, J.-P. Andersen, H. Sun, X. Liu, N. Sonenberg, J. Nie, Y. Shi, *EMBO Rep.* **2020**, *21*, e49898.

[21] J.-P. Andersen, J. Zhang, H. Sun, X. Liu, J. Liu, J. Nie, Y. Shi, *Mol. Metab.* **2020**, *42*, 101055.

[22] X. Xiao, Y. Kim, B. Romartinez-Alonso, K. Sirvydis, D. S. Ory, J. W. R. Schwabe, M. E. Jung, P. Tontonoz, *Proc. Natl. Acad. Sci.* **2021**, *118*, e2024149118.

[23] R. Pedrosa, J. M. Andrés, R. Manzano, C. Pérez-López, *Tetrahedron Lett.* **2013**, *54*, 3101–3104.

[24] B. Bradshaw, G. Etxebarría-Jardi, J. Bonjoch, S. F. Viózquez, G. Guillena, C. Nájera, *Adv. Synth. Catal.* **2009**, *351*, 2482–2490.

[25] H. An, S.-J. Eum, M. Koh, S. K. Lee, S. B. Park, *J. Org. Chem.* **2008**, *73*, 1752–1761.

[26] F. Parhami, E. Jung, Michael, R. Dwyer, Jennifer, K. Nyuyen, *Oxysterol Compounds and the Hedgehog Pathway*, **2007**, WO2007098281 (A2).

[27] D. Samaha, H. H. Hamdo, X. Cong, F. Schumacher, S. Banhart, Ö. Aglar, H. M. Möller, D. Heuer, B. Kleuser, E. M. Saied, C. Arenz, *Chem. Eur. J.* **2020**, *26*, 16616–16621.

10.1002/anie.202111639

WILEY-VCH

RESEARCH ARTICLE

## Entry for the Table of Contents

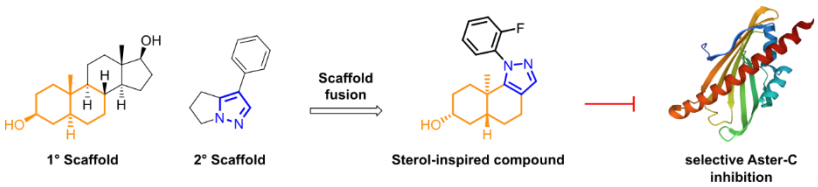


A general strategy for the identification of selective cholesterol transport protein inhibitors through the synthesis of a diverse sterol-inspired compound collection is presented. Fusion of a primary sterol scaffold to diverse secondary natural product-derived scaffolds afforded hits against all of the Aster family of cholesterol transport proteins and selective inhibitors of Aster-C.

Institute and/or researcher Twitter usernames: @laraialab and @tomeveriss and @ChemistryDtu